

1 Ancestral process for infectious disease outbreaks with superspreading

2 Xavier Didelot^{1,2,*}, David Helekal³, Ian Roberts²

3 ¹ School of Life Sciences, University of Warwick, Coventry, United Kingdom

4 ² Department of Statistics, University of Warwick, Coventry, United Kingdom

5 ³ Department of Immunology and Infectious Diseases, Harvard T. H. Chan School of Public Health,
6 Boston, Massachusetts, USA

7 * Corresponding author. Tel: 0044 (0)2476 572827. Email: `xavier.didelot@gmail.com`

8 Running title: Ancestry for outbreaks with superspreading

9 Keywords: infectious disease epidemiology modelling; offspring distribution; superspreading;
10 outbreaks; lambda-coalescent model; multiple mergers

Abstract

When an infectious disease outbreak is of relatively small size, describing the ancestry of a sample of infected individuals is difficult because most ancestral models assume large population sizes. Given a set of sampled individuals, we show that it is possible to express exactly the probability that a subset of them have the same infector, either inclusively (so that other sampled individuals may have the same infector too) or exclusively (so that they may not). To compute these probabilities requires knowledge of the offspring distribution, which determines how many infections each infected individual causes. We consider transmission both without and with superspreading, in the form of a Poisson and Negative-Binomial offspring distribution, respectively. We show how our results can be incorporated into a new lambda-coalescent model which allows multiple lineages to coalesce together. We call this new model the omega-coalescent. We compare it with previously proposed alternatives, and advocate the use of the omega-coalescent for future studies of small outbreaks.

1 Introduction

An outbreak of an infectious disease typically starts when a single or a small number of infected individuals appear within a susceptible population. Each infected individual may come in contact and infect each of the susceptible individuals, who will then become infected in their turn and spread the disease further. Most infectious disease modelling theory describes situations where the disease is at an equilibrium, when the number of infected individuals is high and/or with a significant part of the population already infected (Anderson and May 1991; Keeling and Rohani 2008). Here however we focus on the early stages of an epidemic, where the number of infected individuals is small and the number of susceptibles relatively high and unchanging. In this situation it is useful to think about the number of infections that each newly infected individual is likely to cause, and the probabilistic distribution for this number is often called the offspring distribution (Grassly and Fraser 2008). The mean of the offspring distribution is called the basic reproduction number R_0 and has been given much attention especially since it determines how likely the outbreak is to spread, and how much effort would be needed to bring it under control (Fraser et al. 2004; Ferguson et al. 2006).

If we consider that all individuals are infectious for the same duration and with the same infectiousness, the offspring distribution is Poisson distributed with mean R_0 , which means that the variance of the offspring distribution is also R_0 . We would then say that there is no transmission heterogeneity. However, in practice there are many reasons why this may not be the case, with some individuals being infectious for longer, or being more infectious than others, or having more contacts with susceptibles, or being less symptomatic and therefore less likely to reduce contact numbers, etc. All these factors cause the offspring distribution to be more dispersed than it would otherwise be, that is to have a variance greater than its mean R_0 . A frequent choice to capture this overdispersion is to model the offspring distribution using a Negative-Binomial distribution with mean R_0 and dispersion parameter r (Lloyd-Smith et al. 2005; Grassly and Fraser 2008). When r is close to zero the variance is high compared to the mean, whereas when r is high the variance becomes close to the mean. This transmission heterogeneity is often called superspreading, although this is perhaps misleading as it is the rule rather than the exception of how infectious diseases spread. Superspreading has indeed been described in many diseases (Woolhouse et al. 1997; Stein 2011; Kucharski and Althaus 2015; Wang et al. 2021), and most recently for SARS-CoV-2 (Wang et al. 2020; Lemieux et al. 2021; Gómez-Carballa et al. 2021; Du et al. 2022).

As an outbreak unfolds forward-in-time, a transmission tree is generated representing who-infected-whom, in which each node is an infected individual and points towards a number of nodes distributed

55 according to the offspring distribution. Here we consider the reverse problem of the transmission
 56 ancestry, going backward-in-time, from a sample of infected individuals, until reaching the last common
 57 transmission ancestor of the whole sample. Given a sample of n sampled individuals, we show how
 58 to calculate the probability that a given subset of size k have the same infector, either inclusively (so
 59 that the remaining $n - k$ may also have the same infector or not) or exclusively (so that none of the
 60 remaining $n - k$ have the same infector). We start by considering the general case of an offspring
 61 distribution with arbitrary form, and then the specific cases of offspring distributions that follow a
 62 Poisson or a Negative-Binomial distribution. The main novelty of our approach is that we consider that
 63 the overall population size is small, but we show that if the population size is large, our results agree
 64 with several previous studies (Volz 2012; Koelle and Rasmussen 2012; Fraser and Li 2017). Finally, we
 65 show how our results can be incorporated into a new lambda-coalescent model (Pitman 1999; Sagitov
 66 1999; Donnelly and Kurtz 1999) and compare it with previously described models.

67 2 General case

68 Let time be measured in discrete units and denoted t . Each discrete value of t correspond to a unique
 69 non-overlapping generations of infected individuals, so that individuals infected at t will have offspring
 70 at $t + 1$, etc. Let N_t denote the number of infectious individuals at time t . Each of them creates a
 71 number $s_{t,i}$ of secondary infections at time $t + 1$, following the offspring distribution $\alpha_t(s)$. The mean
 72 of this distribution is the basic reproduction number R_t and the variance is V_t . We have:

$$N_{t+1} = \sum_{i=1}^{N_t} s_{t,i} \quad (1)$$

73 2.1 Inclusive coalescence probability

74 We define the inclusive coalescence probability $p_{k,t}(N_t, N_{t+1})$ as the probability that a specific set of
 75 k individuals from generation $t + 1$ find a common ancestor in generation t , conditional on population
 76 sizes N_t and N_{t+1} .

77 Given full information about offspring counts from individuals in generation t , $\mathbf{s}_t = (s_{t,1}, \dots, s_{t,N_t})$, we
 78 have

$$\begin{aligned}
p_{k,t}(\mathbf{s}_t, N_t) &= \sum_{i=1}^{N_t} \frac{\binom{s_{t,i}}{k}}{\binom{N_{t+1}}{k}} \\
&= \sum_{i=1}^{N_t} \frac{\Gamma(s_{t,i} + 1) \Gamma(N_{t+1} - k + 1)}{\Gamma(s_{t,i} - k + 1) \Gamma(N_{t+1})}
\end{aligned} \tag{2}$$

79

80 Full information $\{s_{t,i}\}$ yields the population size N_{t+1} but is not feasible to observe in practice. We
81 can instead express the inclusive coalescence probability conditioning on the next population size N_{t+1}
82 by summing over possible offspring counts $\mathbf{s}_t = (s_{t,1}, \dots, s_{t,N_t})$ conditional on the total generation size.
83 Let $S_t^{-(1)} = (S_{t,2}, \dots, S_{t,N_t})$.

$$\begin{aligned}
p_{k,t}(N_t, N_{t+1}) &= \sum_{\mathbf{s}_t \in \mathbb{N}_0^{N_t}} \mathbb{P} \left[\mathbf{S}_t = \mathbf{s}_t \mid \sum_{i=1}^{N_t} S_{t,i} = N_{t+1} \right] p_{k,t}(\mathbf{s}_t, N_t) \\
&= \sum_{\mathbf{s}_t \in \mathbb{N}_0^{N_t}} \mathbb{P} \left[\mathbf{S}_t = \mathbf{s}_t \mid \sum_{i=1}^{N_t} S_{t,i} = N_{t+1} \right] \sum_{i=1}^{N_t} \frac{\binom{s_{t,i}}{k}}{\binom{N_{t+1}}{k}} \\
&= \sum_{i=1}^{N_t} \sum_{\mathbf{s}_t \in \mathbb{N}_0^{N_t}} \frac{\binom{s_{t,i}}{k}}{\binom{N_{t+1}}{k}} \mathbb{P} \left[S_{t,1} = s_{t,1}, \mathbf{s}_t^{-(1)} = \mathbf{s}_t^{-(1)} \mid \sum_{i=1}^{N_t} S_{t,i} = N_{t+1} \right] \\
&= \frac{N_t}{\binom{N_{t+1}}{k}} \sum_{\mathbf{s}_t \in \mathbb{N}_0^{N_t}} \binom{s_{t,1}}{k} \mathbb{P} \left[S_{t,1} = s_{t,1} \mid \sum_{i=1}^{N_t} S_{t,i} = N_{t+1} \right] \\
&\quad \times \mathbb{P} \left[\mathbf{s}_t^{-(1)} = \mathbf{s}_t^{-(1)} \mid S_{t,1} = s_{t,1}, \sum_{i=1}^{N_t} S_{t,i} = N_{t+1} \right] \\
&= \frac{N_t}{\binom{N_{t+1}}{k}} \sum_{s_{t,1}=0}^{N_{t+1}} \binom{s_{t,1}}{k} \mathbb{P} \left[S_{t,1} = s_{t,1} \mid \sum_{i=1}^{N_t} S_{t,i} = N_{t+1} \right] \\
&\quad \times \underbrace{\sum_{\mathbf{s}_t^{-(1)} \in \mathbb{N}_0^{N_t-1}} \mathbb{P} \left[\mathbf{s}_t^{-(1)} = \mathbf{s}_t^{-(1)} \mid \sum_{i=2}^{N_t} S_{t,i} = N_{t+1} - s_{t,1} \right]}_{=1} \\
&= \frac{N_t}{\binom{N_{t+1}}{k}} \mathbb{E} \left[\binom{S_{t,1}}{k} \mid \sum_{i=1}^{N_t} S_{t,i} = N_{t+1} \right]
\end{aligned} \tag{3}$$

84

85 The k -th falling factorial moments $\mathbb{E} \left[\frac{S_{t,1}!}{(S_{t,1}-k)!} \mid \sum_{i=1}^{N_t} S_{t,i} = N_{t+1} \right]$ in Equation 3 can be readily obtained

86 by differentiating the probability generating function of $S_{t,1} | (\sum_{i=1}^{N_t} S_{t,i} = N_{t+1})$.

87 2.2 Exclusive coalescence probability

88 Generally, we observe a sample of individuals from each generation rather than the entire population.
 89 In this case, we are interested in the exclusive coalescence probability $p_{n,k,t}(N_t, N_{t+1})$ that exactly k
 90 individuals from a sample of n arose from a common ancestor one generation in the past given knowlege
 91 of the total population sizes N_t and N_{t+1} .

92 Given full information about offspring counts of the parents of sampled individuals at the present,
 93 $\mathbf{x}_t = (x_{t,1}, \dots, x_{t,N_t})$, we have

$$\begin{aligned} p_{n,k,t}(\mathbf{x}_t, N_t) &= \sum_{i=1}^{N_t} \frac{\binom{x_{t,i}}{k}}{\binom{n}{k}} \mathbb{I}\{x_{t,i} = k\} \\ &= \sum_{i=1}^{N_t} \frac{x_{t,i}!}{(x_{t,i} - k)!} \frac{(n - k)!}{n!} \mathbb{I}\{x_{t,i} = k\} \end{aligned} \quad (4)$$

94 Similarly to the exclusive coalescence probability, we can use this to evaluate the exclusive probability
 95 given N_t and N_{t+1} by summing over possible parent offspring configurations (for $k \leq n$),

$$\begin{aligned}
p_{n,k,t}(N_t, N_{t+1}) &= \sum_{\mathbf{x}_t \in \mathbb{N}_0^{N_t}} \mathbb{P} \left[\mathbf{X}_t = \mathbf{x}_t \middle| \sum_{i=1}^n X_{t,i} = n \right] p_{n,k,t}(\mathbf{x}_t, N_t) \\
&= \sum_{\mathbf{x}_t \in \mathbb{N}_0^{N_t}} \mathbb{P} \left[\mathbf{X}_t = \mathbf{x}_t \middle| \sum_{i=1}^n X_{t,i} = n \right] \sum_{i=1}^{N_t} \frac{\binom{x_{t,i}}{k}}{\binom{n}{k}} \mathbb{I}\{x_{t,i} = k\} \\
&= \frac{N_t}{\binom{n}{k}} \sum_{\mathbf{x}_t \in \mathbb{N}_0^{N_t}} \binom{x_{t,1}}{k} \mathbb{P} \left[\mathbf{X}_t = \mathbf{x}_t \middle| \sum_{i=1}^{N_t} X_{t,i} = n \right] \mathbb{I}\{x_{t,1} = k\} \\
&= \frac{N_t}{\binom{n}{k}} \sum_{\mathbf{x}_t^{-(1)} \in \mathbb{N}_0^{N_t-1}} \binom{k}{k} \mathbb{P} \left[X_{t,1} = k, \mathbf{X}_t^{-(1)} = \mathbf{x}_t^{-(1)} \middle| \sum_{i=1}^{N_t} X_{t,i} = n \right] \\
&= \frac{N_t}{\binom{n}{k}} \mathbb{P}[X_{t,1} = k \middle| \sum_{i=1}^{N_t} X_{t,i} = n] \underbrace{\sum_{\mathbf{x}_t^{-(1)} \in \mathbb{N}_0^{N_t-1}} \mathbb{P} \left[\mathbf{X}_t^{-(1)} = \mathbf{x}_t^{-(1)} \middle| \sum_{i=1}^{N_t} X_{t,i} = n, X_{t,1} = k \right]}_{=1} \\
&= \frac{N_t}{\binom{n}{k}} \mathbb{P} \left[X_{t,1} = k \middle| \sum_{i=1}^{N_t} X_{t,i} = n \right] \tag{5}
\end{aligned}$$

96 Note that $X_{t,i}$ does not follow the same offspring distribution as $S_{t,i}$. $(X_{t,1}, \dots, X_{t,N_t})$ consists of n
 97 individuals sampled from generation $t+1$ without replacement - there is no guarantee that all offspring
 98 from any given parent are included in the sample.

99 **2.3 Complementarity of exclusive coalescence probabilities**

100 If we consider one of the lines observed amongst a set of n , it can either remain uncoalesced (with
 101 probability $p_{n,1,t}$) or coalesce in an event of size k (with probability $p_{n,k,t}$) with any set of $k-1$ lines
 102 among the $n-1$ other lines, leading to the following complementarity equation:

$$\sum_{k=1}^n \binom{n-1}{k-1} p_{n,k,t} = 1 \tag{6}$$

103 We can show that it is indeed satisfied by the formula in Equation 5:

$$\begin{aligned}
\sum_{k=1}^n \binom{n-1}{k-1} p_{n,k,t} &= \sum_{k=1}^n \binom{n-1}{k-1} \frac{N_t}{\binom{n}{k}} \mathbb{P} \left[X_1 = k \middle| \sum_{i=1}^{N_t} X_i = n \right] \\
&= \sum_{k=1}^n N_t \frac{k}{n} \mathbb{P} \left[X_1 = k \middle| \sum_{i=1}^{N_t} X_i = n \right] \\
&= \frac{N_t}{n} \sum_{k=0}^n k \mathbb{P} \left[X_1 = k \middle| \sum_{i=1}^{N_t} X_i = n \right] \\
&= \frac{N_t}{n} \mathbb{E} \left[X_1 \middle| \sum_{i=1}^{N_t} X_i = n \right] \\
&= \frac{1}{n} \sum_{i=1}^{N_t} \mathbb{E} \left[X_i \middle| \sum_{i=1}^{N_t} X_i = n \right] \\
&= \frac{1}{n} \mathbb{E} \left[\sum_{i=1}^{N_t} X_i \middle| \sum_{i=1}^{N_t} X_i = n \right] \\
&= 1
\end{aligned} \tag{7}$$

104 3 Poisson case

105 In this section we consider that the offspring distribution is $\alpha_t = \text{Poisson}(R_t)$. In this case, we have:

$$\sum_{i=1}^{N_t} S_{t,i} \sim \text{Poisson}(N_t R_t) \tag{8}$$

106 and the conditional distribution:

$$\begin{aligned}
\mathbb{P} \left[S_{t,1} = s \middle| \sum_{i=1}^{N_t} S_{t,i} = N_{t+1} \right] &= \frac{\mathbb{P} \left[S_{t,1} = s, \sum_{i=1}^{N_t} S_{t,i} = N_{t+1} \right]}{\mathbb{P} \left[\sum_{i=1}^{N_t} S_{t,i} = N_{t+1} \right]} \\
&= \frac{\alpha_t(s) \mathbb{P} \left[\sum_{i=2}^{N_t} S_{t,i} = N_{t+1} - s \right]}{\mathbb{P} \left[\sum_{i=1}^{N_t} S_{t,i} = N_{t+1} \right]} \\
&= \frac{\frac{R_t^s e^{-R_t}}{s!} \cdot \frac{((N_t - 1)R_t)^{N_{t+1}-s}}{(N_{t+1} - s)!}}{\frac{(N_t R_t)^{N_{t+1}} e^{-N_t R_t}}{N_{t+1}!}}
\end{aligned}$$

$$= \binom{N_{t+1}}{s} \left(\frac{1}{N_t}\right)^s \left(1 - \frac{1}{N_t}\right)^{N_{t+1}-s} \quad (9)$$

107

108 This is the probability mass function of a Binomial distribution and therefore we deduce that:

$$S_{t,1} \left| \left(\sum_{i=1}^{N_t} S_{t,i} = N_{t+1} \right) \right. \sim \text{Binomial} \left(N_{t+1}, \frac{1}{N_t} \right) \quad (10)$$

109 The k -th falling factorial moments of $X \sim \text{Binomial}(n, p)$ are (Potts 1953):

$$\mathbb{E} \left[\frac{X!}{(X-k)!} \right] = \binom{n}{k} p^k k! \quad (11)$$

110 By applying this formula to the Binomial distribution in Equation 10 and injecting into Equation 3
 111 we obtain the inclusive probability of coalescence for k lines:

$$\mathbb{E} \left[\binom{S_{t,1}}{k} \left| \sum_{i=1}^{N_t} S_{t,i} = N_{t+1} \right. \right] = \frac{1}{k!} \mathbb{E} \left[\frac{S_{t,1}!}{(S_{t,1}-k)!} \left| \sum_{i=1}^{N_t} S_{t,i} = N_{t+1} \right. \right] = \frac{1}{k!} \frac{N_{t+1}!}{(N_{t+1}-k)!} \left(\frac{1}{N_t} \right)^k \quad (12)$$

112 Consequently, the inclusive probability of coalescence for k lines is

$$p_{k,t} = \frac{1}{N_t^{k-1}} \quad (13)$$

113 By injecting the probability mass function of the Binomial distribution in Equation 10 into Equation
 114 5 we deduce that the exclusive probability of coalescence for k lines from a sample of n ($n \geq k$) is

$$p_{n,k,t} = \frac{(N_t - 1)^{n-k}}{N_t^{n-1}} \quad (14)$$

115 It is interesting to note that neither the inclusive nor the exclusive coalescence probability depend on
 116 the mean R_t of the Poisson offspring distribution or the size N_{t+1} of the population at time $t+1$. The
 117 inclusive coalescent probability in Equation 13 can also be obtained conceptually by considering that
 118 among the k lines, the first one has an ancestor with probability one, and the remaining $k-1$ need to
 119 have the same ancestor among a set of N_t from which they choose uniformly at random so that the

120 probability of picking the same ancestor is $1/N_t$. The exclusive coalescent probability in Equation 14
 121 can be derived likewise by considering that in addition to the above, each of the $n - k$ other lines need
 122 to choose a different ancestor, which happens with probability $(N_t - 1)/N_t$.

123 Figure 1 illustrates the inclusive and exclusive coalescence probabilities for the Poisson case for a set
 124 of size $k = 1$ to $k = 10$ amongst a total of $n = 10$ observed lines, in a population of size $N_t = 10$,
 125 $N_t = 20$ or $N_t = 30$.

126 4 Negative-Binomial case

127 In this section we consider that the offspring distribution is $\alpha_t = \text{Negative-Binomial}(r, p)$ with
 128 parameters (r, p) set by moment-matching mean R_t and variance V_t which are assumed constant
 129 over time. The resulting parameters for this distribution are $r = R_t^2/(V_t - R_t)$ and $p = R_t/V_t$. In this
 130 case, we have:

$$\sum_{i=1}^{N_t} S_{t,i} \sim \text{Negative-Binomial}(N_t r, p) \quad (15)$$

131 and similarly to the Poisson(λ) offspring distribution identify the conditional distribution of
 132 $S_{t,1} | \sum_{i=1}^{N_t} S_{t,i}$ is as follows:

$$\begin{aligned} \mathbb{P}\left[S_{t,1} = s \mid \sum_{i=1}^{N_t} S_{t,i} = N_{t+1}\right] &= \frac{\alpha_t(s) \cdot \mathbb{P}\left[\sum_{i=2}^{N_t} S_{t,i} = N_{t+1} - s\right]}{\mathbb{P}\left[\sum_{i=1}^{N_t} S_{t,i} = N_{t+1}\right]} \\ &= \frac{\frac{\Gamma(r+s)}{s!\Gamma(r)}(1-p)^s p^r \cdot \frac{\Gamma((N_t-1)r + (N_{t+1}-s))}{(N_{t+1}-s)!\Gamma((N_t-1)r)}(1-p)^{N_{t+1}-s} p^{(N_t-1)r}}{\frac{\Gamma(N_t r + N_{t+1})}{N_{t+1}!\Gamma(N_t r)}(1-p)^{N_{t+1}} p^{N_t r}} \\ &= \frac{N_{t+1}!}{s!(N_{t+1}-s)!} \frac{\Gamma(r+s)\Gamma((N_t-1)r + (N_{t+1}-s))}{\Gamma(N_t r + N_{t+1})} \frac{\Gamma(N_t r)}{\Gamma(r)\Gamma((N_t-1)r)} \\ &= \binom{N_{t+1}}{s} \frac{B(s+r, N_{t+1}-s+(N_t-1)r)}{B(r, (N_t-1)r)} \quad (16) \end{aligned}$$

133

134 where $B(x, y)$ denotes the Beta function defined as $B(x, y) = \Gamma(x)\Gamma(y)/\Gamma(x+y)$. This is the probability
 135 mass function of a Beta-Binomial distribution and therefore we deduce that:

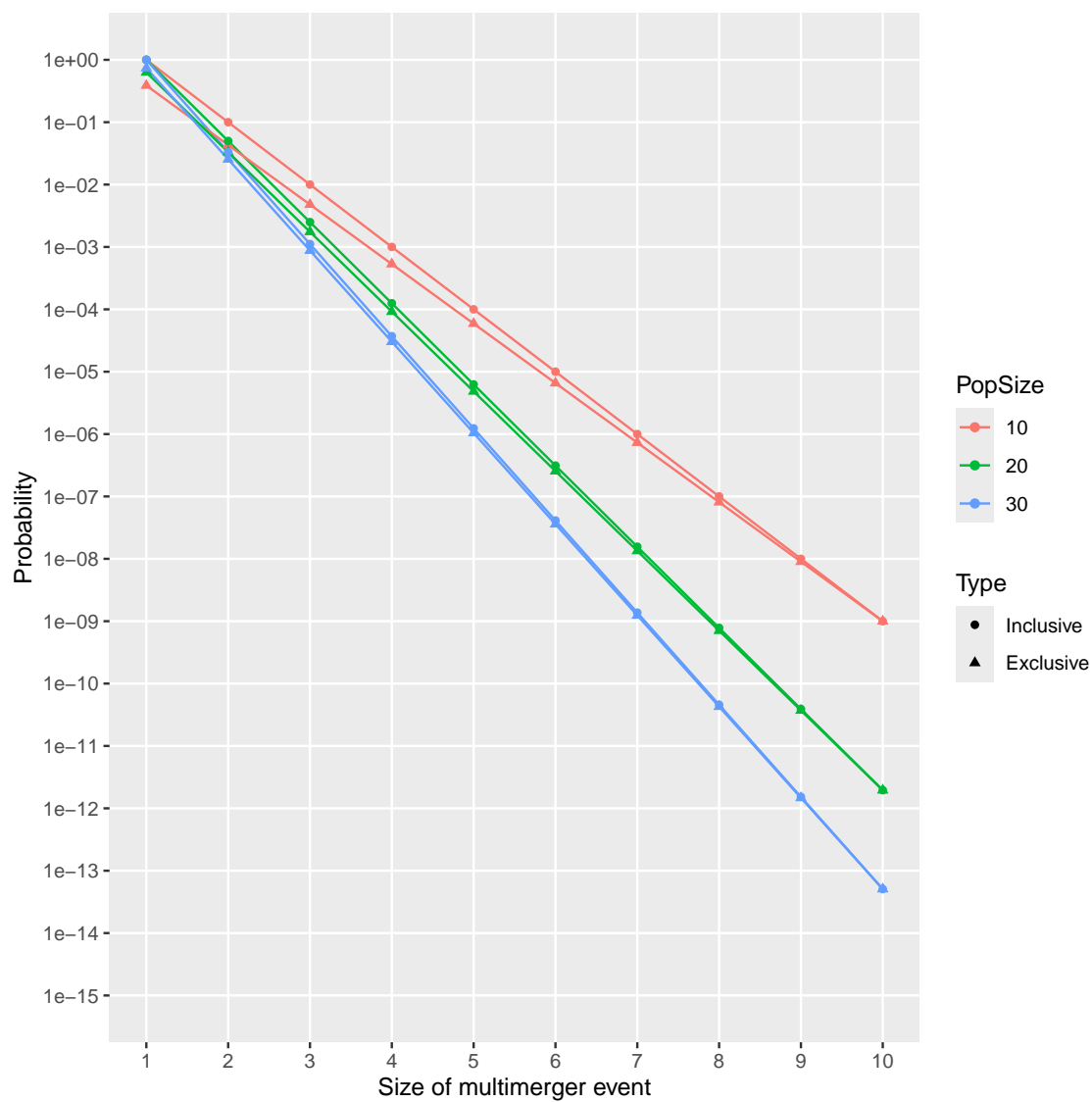


Figure 1: Inclusive and exclusive coalescence probabilities for the Poisson case.

$$S_{t,1} \left| \left(\sum_{i=1}^{N_t} S_{t,i} = N_{t+1} \right) \right. \sim \text{Beta-Binomial}(r, (N_t - 1)r) \quad (17)$$

136 The k -th falling factorial moments of $X \sim \text{Beta-Binomial}(\alpha, \beta)$ are (Tripathi et al. 1994):

$$\mathbb{E} \left[\frac{X!}{(X-k)!} \right] = \binom{n}{k} \frac{B(\alpha + k, \beta)k!}{B(\alpha, \beta)} \quad (18)$$

137 By applying this formula to the Beta-Binomial distribution in Equation 17 and injecting into Equation
138 3, we deduce that the inclusive probability of coalescence for k lines is:

$$p_{k,t} = \frac{B(N_t r + 1, r + k)}{B(r + 1, N_t r + k)} \quad (19)$$

139 By injecting the probability mass function of the Beta-Binomial distribution in Equation 17 into
140 Equation 5 we deduce that the exclusive probability of coalescence for k lines is:

$$p_{n,k,t} = \frac{N_t B(k + r, n - k + N_t r - r)}{B(r, N_t r - r)} \quad (20)$$

141 It is interesting to note that as for the Poisson case, the inclusive and exclusive coalescence probabilities
142 do not depend on the size N_{t+1} of the population at time $t + 1$. They both depend on the Negative-
143 Binomial offspring distribution only through the dispersion parameter r . If we consider that r is large
144 in Equations 19 and 20, we can derive that the asymptotic behaviour is the same as in the Poisson
145 case shown in Equations 13 and 14. For example this can be derived by rewriting the Beta functions
146 using Gamma functions, and using the following form of Stirling's approximation:

$$\lim_{a \rightarrow \infty} \frac{\Gamma(a + b)}{\Gamma(a)} = a^b e^{-b} \quad (21)$$

147 Figure 2 illustrates the inclusive and exclusive coalescence probabilities for the Negative-Binomial case
148 for a set of size $k = 1$ to $k = 10$ amongst a total of $n = 10$ observed lines, in a population of size
149 $N_t = 12$. Several Negative-Binomial offspring distributions are compared, all of which have the same
150 mean $R_t = 2$, and with the dispersion parameter equal to $r = 1$, $r = 2$, $r = 10$ and $r = 100$. When

151 $r = 1$ the Negative-Binomial reduces to a Geometric distribution. When r is high (for example $r = 100$
 152 as shown in Figure 2) the dispersion is low and the Negative-Binomial case behaves almost like the
 153 Poisson case. When r is lower the dispersion of the offspring distribution increases, so that both the
 154 inclusive and exclusive probabilities of larger multimerger events increase.

155 5 Limit when the population size is large

156 If we consider that the population size N_t is fixed and large, we can show the connections between our
 157 results and several previous studies. In the Poisson case, from Equations 13 and 14 we can see that
 158 both inclusive and exclusive probabilities are of order $\mathcal{O}(N_t^{1-k})$. We can therefore ignore events with
 159 $k > 2$ and retain only the events with $k = 2$ which occur with probability:

$$p_{2,t} = p_{n,2,t} = \frac{1}{N_t} \quad (22)$$

160 For the Negative-Binomial case, from Equations 19 and 20 we can rewrite using Gamma functions
 161 and apply the form of Stirling's equation given in Equation 21 to show that once again both inclusive
 162 and exclusive probabilities are also of order $\mathcal{O}(N_t^{1-k})$. We can therefore once again ignore events with
 163 $k > 2$ and retain only the events with $k = 2$ which occur with probability:

$$p_{2,t} = p_{n,2,t} = \frac{r+1}{N_t r + 1} \approx \frac{r+1}{N_t r} \quad (23)$$

164 Koelle and Rasmussen (2012) derived the rates of coalescence of two lineages for several epidemiological
 165 models, assuming a large population at equilibrium. For each model they use the equation $N_e = N/\sigma^2$
 166 to relate the effective population size N_e to the actual population size N and the variance σ^2 in the
 167 number of offspring. This relationship was first established by Kingman (1982a) to derive the backward-
 168 in-time coalescent model from the forward-in-time Cannings exchangeable models (Cannings 1974).
 169 From Equation 23 we can take $R_t = 1$ to achieve equilibrium of the population size and the method
 170 of moments estimator $r = R_t^2/(V_t - R_t) = 1/(V_t - 1)$ to deduce the equivalent $p_{2,t} = V_t/N_t$.

171 Volz (2012) showed that the rate of coalescence for two lineages under a continuous-time epidemic
 172 coalescent model is $2f(t)/I(t)^2$ where $f(t)$ is the incidence and $I(t)$ the prevalence. Setting in this
 173 formula the prevalence as $I(t) = N_{t+1} = N_t R_t$ and the incidence as $f(t) = R_t N_{t+1} = R_t^2 N_t$ we get a

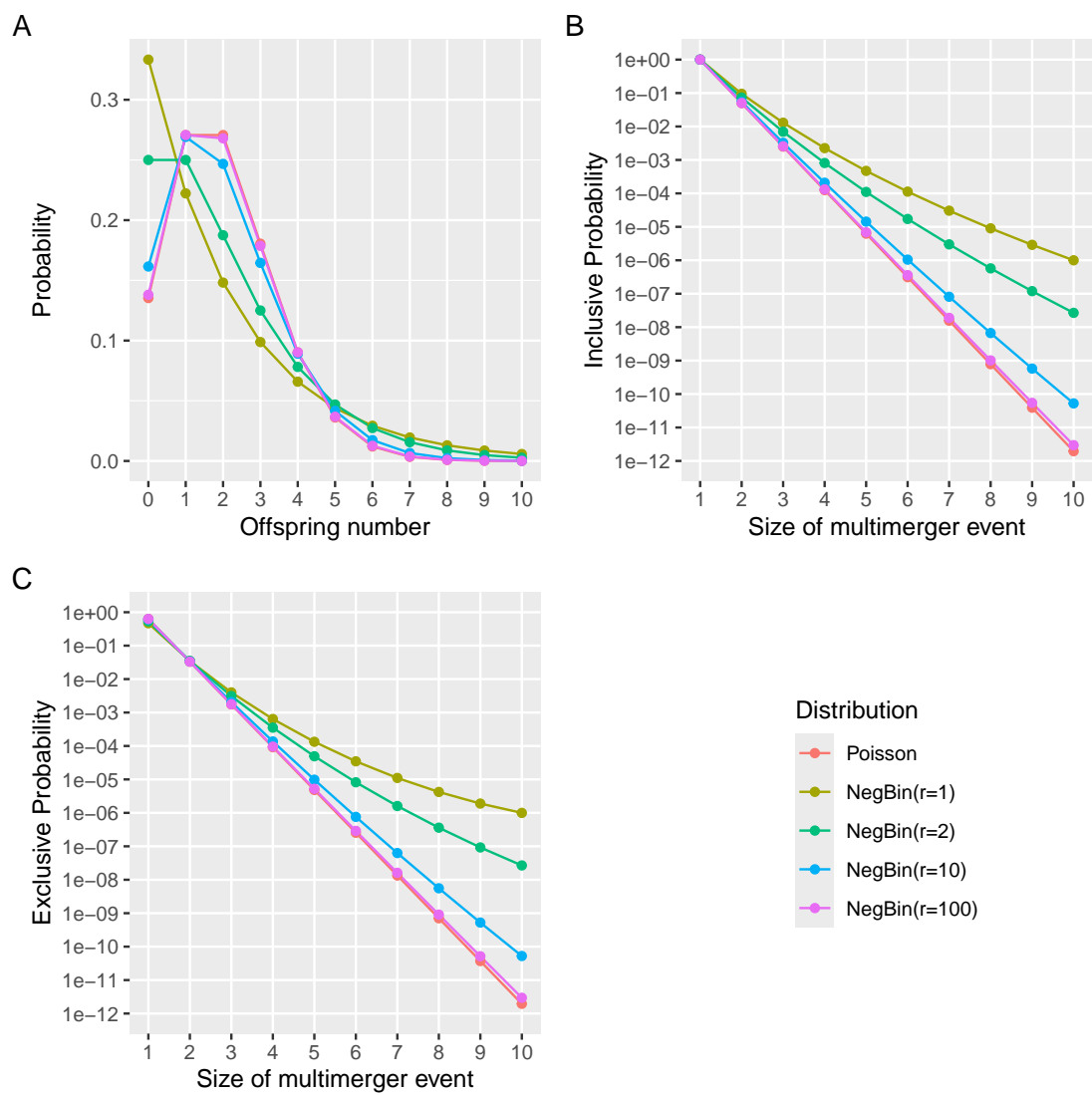


Figure 2: (A) Offspring distribution. (B) Inclusive probability of coalescence. (C) Exclusive probability of coalescence.

174 coalescent rate of $2/N_t$. To apply our methodology we need to consider that the offspring distribution
 175 is Geometric, since the epidemiological models considered have successes (offspring) happening until
 176 the first failure (removal). We therefore set $r = 1$ in Equation 23 to make the Negative-Binomial
 177 offspring distribution reduce to a Geometric distribution and the same result follows.

178 Fraser and Li (2017) calculated the effective population size $N_e(t)$ as a function of the actual population
 179 size $N(t)$ and the mean and variance of the offspring distribution R and σ^2 . This formula was used to
 180 estimate the dispersion parameter of a Negative-Binomial offspring distribution from genetic data (Li
 181 et al. 2017). In our notation, their formula is equivalent to:

$$p_{2,t} = \frac{V_t/R_t + R_t - 1}{N_t R_t} \quad (24)$$

182 In the Poisson case we have $V_t = R_t$ so that Equation 24 simplifies to $p_{2,t} = 1/N_t$ which agrees with
 183 Equation 22. In the Negative-Binomial case we have $V_t/R_t = 1/p = (r + R_t)/r$ so that Equation 24
 184 simplifies to $(r + 1)/(N_t r)$ which agrees with our Equation 23. Conversely, if we substitute the method
 185 of moments estimator $r = R_t^2/(V_t - R_t)$ in Equation 23 we obtain the Equation 24.

186 6 Definition of a new lambda-coalescent model

187 The coalescent model (Kingman 1982a,b) describes the ancestry of a sample from a large population
 188 evolving according to many forward-in-time models such as the Wright-Fisher model (Wright 1931;
 189 Fisher 1930), the Moran model (Moran 1958) and the Cannings exchangeable model (Cannings 1974).
 190 Since the coalescent considers a large population in which each individual only has a number of
 191 offspring that is small compared to the population size, coalescent trees are always binary and do not
 192 feature multimergers, making them unsuitable to represent the ancestry of outbreaks considered in
 193 this study. However, the lambda-coalescent models are an extension of the coalescent model that do
 194 allow multimergers (Pitman 1999; Sagitov 1999; Donnelly and Kurtz 1999).

195 A lambda-coalescent model is defined by a probability measure $\Lambda(dx)$ on the interval $[0, 1]$, from which
 196 we can deduce the rate $\lambda_{n,k}$ at which any subset of k lineages within a set of n observed lineages
 197 coalesce:

$$\lambda_{n,k} = \int_0^1 x^{k-2} (1-x)^{n-k} \Lambda(dx) \quad (25)$$

198 The beta-coalescent (Schweinsberg 2003) is a specific type of lambda-coalescent that has been used
 199 recently in several studies analysing genetic data from infectious disease agents (Hoscheit and Pybus
 200 2019; Menardo et al. 2021; Helekal et al. 2025; Zhang and Palacios 2024). The beta-coalescent model
 201 has a single parameter $\alpha \in [0, 2]$ and is defined as:

$$\Lambda(dx) = \frac{x^{1-\alpha} (1-x)^{\alpha-1}}{B(2-\alpha, \alpha)} dx \quad (26)$$

202 By combining Equations 25 and 26 we can deduce that:

$$\lambda_{n,k} = \frac{B(k-\alpha, n-k+\alpha)}{B(2-\alpha, \alpha)} \quad (27)$$

203 Special cases of the beta-coalescent include $\alpha = 2$ corresponding to the Kingman coalescent, $\alpha = 1$
 204 which is known as the Bolthausen-Sznitman coalescent and $\alpha = 0$ for which the phylogeny is always
 205 star-shaped.

206 We now define a new lambda-coalescent based on the Negative-Binomial case described previously.
 207 We call this new lambda-coalescent model the omega-coalescent (where omega stands for outbreak).
 208 For ease of comparison with other coalescent models, we consider that time is continuous and that
 209 the population size remains constant equal to N_t . The exclusive coalescent probability $p_{n,k,t}$ in the
 210 Negative-Binomial case given by Equation 20 can be used to determine the corresponding rate of the
 211 omega-coalescent, if we consider that the probability of each event in discrete time is the result of the
 212 event happening at a constant rate in continuous time:

$$\lambda_{n,k} = -\log(1 - p_{n,k,t}) \quad (28)$$

213 In order to compare the omega-coalescent defined in Equation 28 with other models such as the beta-
 214 coalescent defined in Equation 27, we consider the distribution of the size k of the next event among
 215 a set of n lineages. For any lambda-coalescent this can be computed as:

$$p(k|n) = \frac{\binom{n}{k} \lambda_{n,k}}{\sum_{i=2}^n \binom{n}{i} \lambda_{n,i}} \quad (29)$$

Figure 3 compares this distribution for $n = 10$ in the beta-coalescent with parameter $\alpha \in \{0.5, 1, 1.5\}$ and for the omega-coalescent with parameters $N_t \in \{15, 25, 50\}$ and $r \in \{0.1, 0.5, 1\}$. In the beta-coalescent, the distribution shifts towards more larger multimerger events as the parameter α decreases. In the omega-coalescent a wider range of behaviours is obtained when varying the two parameters N_t and r . For a given value of N_t , decreasing the value of r results in more larger events. Conversely, for a given value of r we can see that increasing the value of N_t reduces the probability of larger events.

Genealogies can be simulated from the omega-coalescent model defined in Equation 28 using the same algorithm as for other lambda-coalescent models (Pitman 1999). Figure 4 shows examples of trees simulated for a sample of size $n = 20$, constant population size $N_t = 40$ and dispersion parameter $r \in \{0.1, 1, 5, 10\}$. It is already clear from these single realisations that the lower values of r result in trees with more larger multimerger events and lower time to the most recent common ancestor, but to quantify these properties we need to consider many trees.

Figure 5 shows summary statistics for 10,000 trees simulated in the same conditions as the individual trees shown in Figure 4. As the dispersion parameter increases from $r = 0.1$ to $r = 10$ multimerger events become less and less likely and large. Simultaneously, the time to the most recent common ancestor increases, as well as the stemminess of the tree (ie the proportion of branch lengths in non-terminal branches).

7 Parameter inference

Consider a genealogy T with n leaves and c coalescent nodes, with $t_0 = 0$ the sampling time, t_1, \dots, t_c the times of the coalescent nodes in increasing order and k_i the number of lineages coalescing at time t_i . The number of lineages existing between time t_{i-1} and t_i is then $n_i = n - \sum_{j=1}^{i-1} k_j$. Under a lambda-coalescent model, the genealogy T has likelihood:

$$p(T|\Lambda) = \prod_{i=1}^c \lambda_{n_i, k_i} \exp \left(- \sum_{j=2}^{n_i} \binom{n_i}{j} \lambda_{n_i, j} (t_i - t_{i-1}) \right) \quad (30)$$

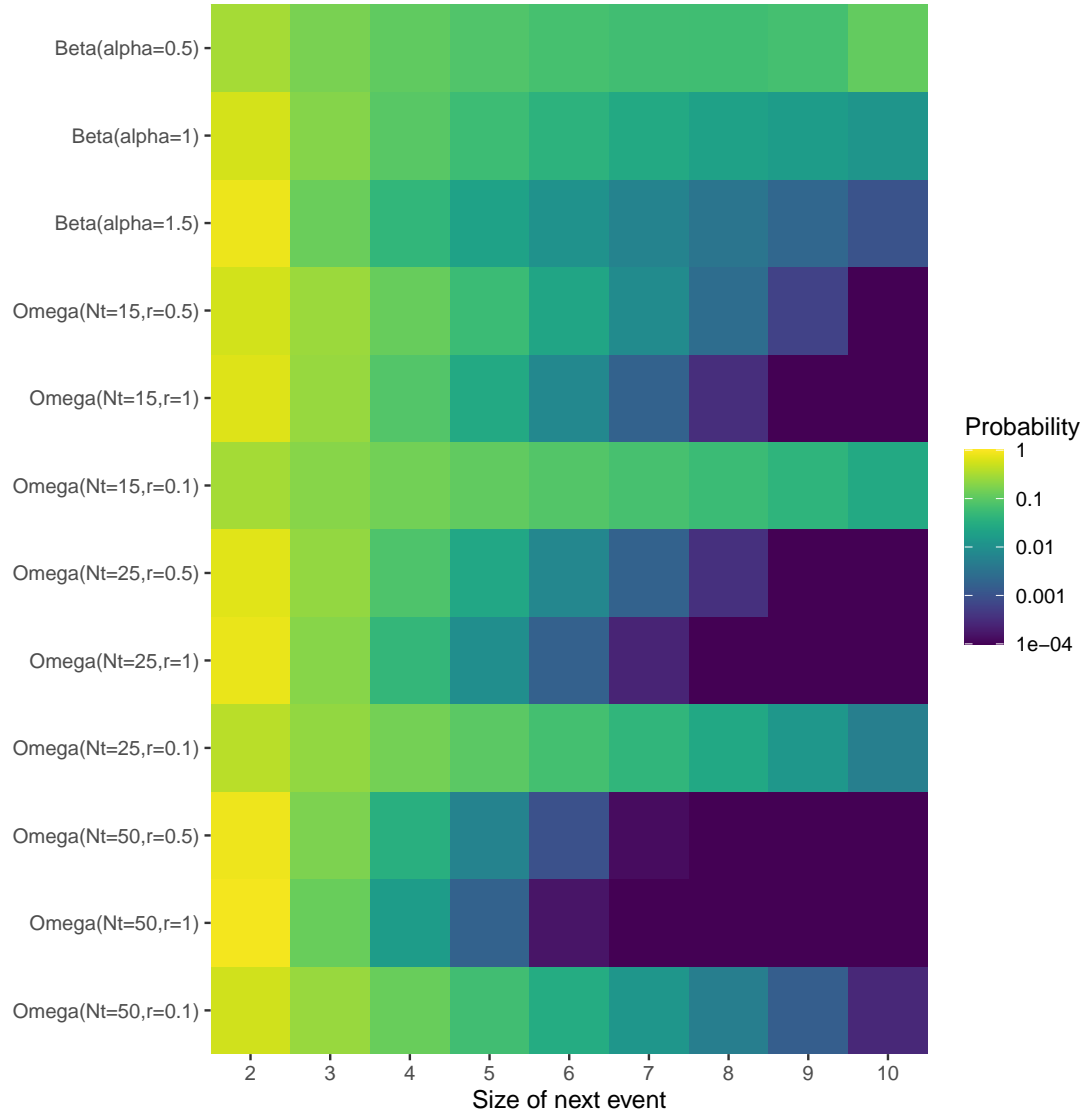


Figure 3: Distribution of the size of the next event among a set of $n = 10$ lineages, compared between the beta-coalescent and the omega-coalescent model with various parameters.

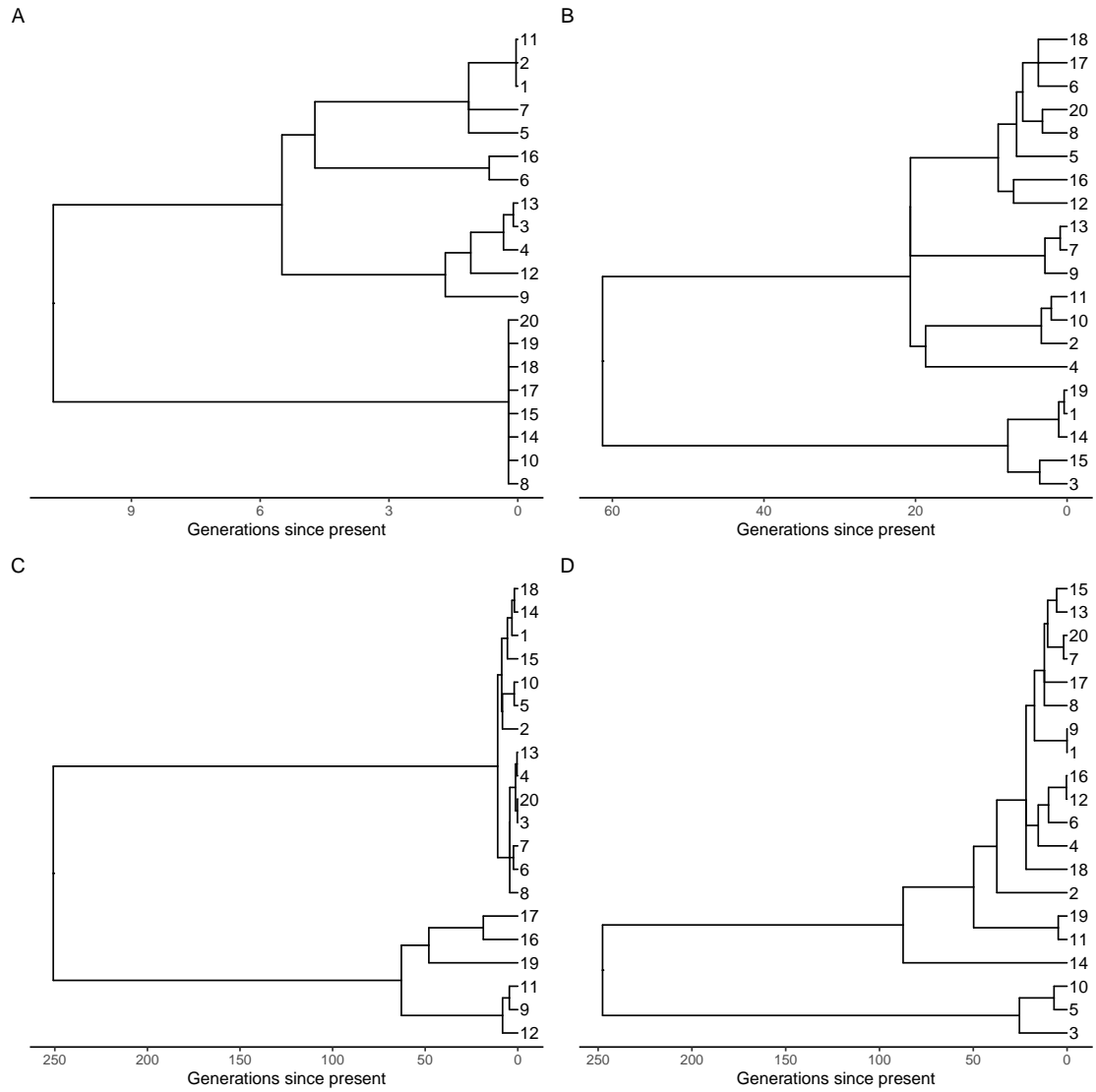


Figure 4: Example of trees simulated under the omega-coalescent with $r = 0.1$ (A), $r = 1$ (B), $r = 5$ (C) and $r = 10$ (D).

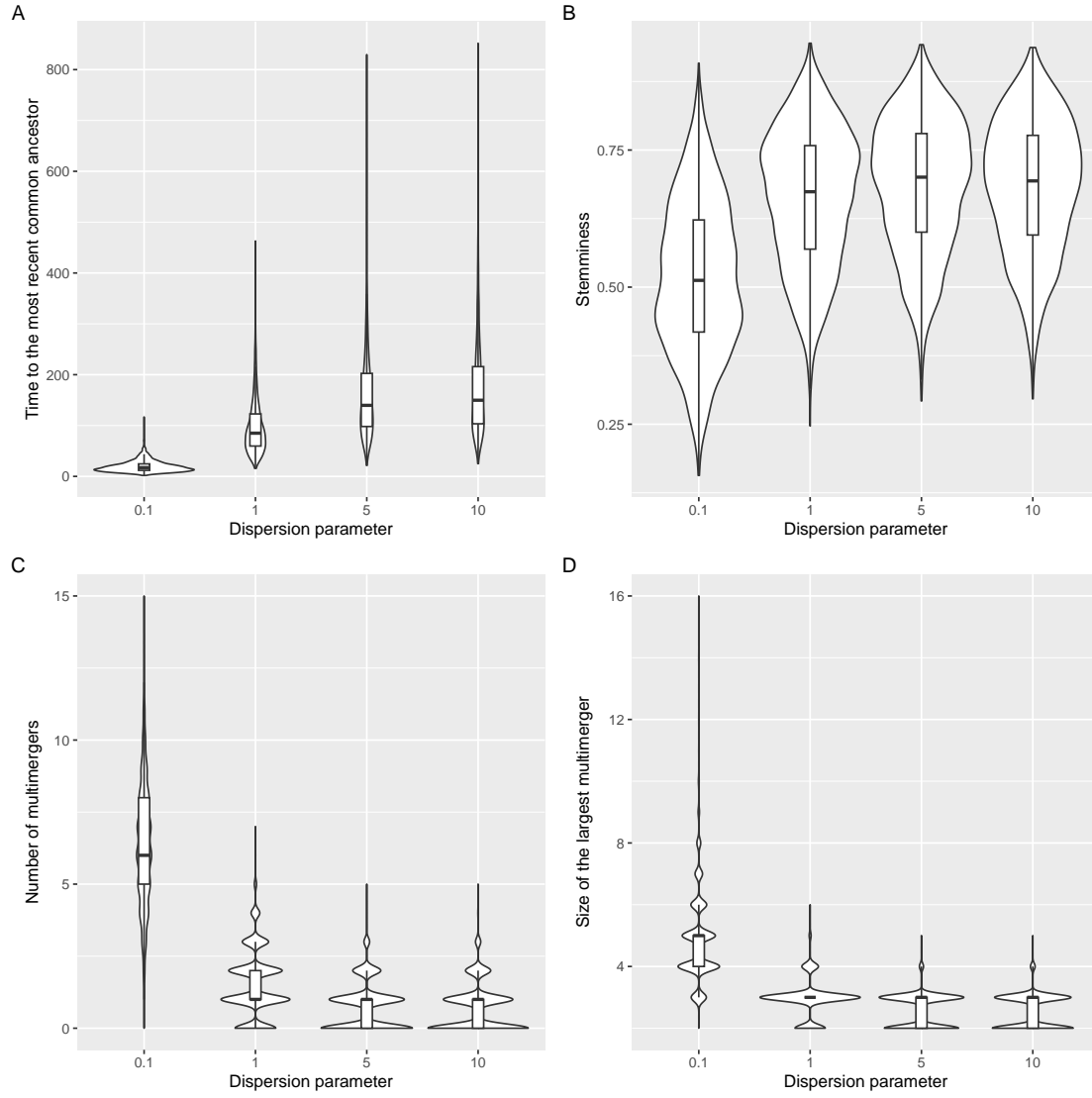


Figure 5: Summary statistics for trees simulated under the omega-coalescent with $r = 0.1, r = 1, r = 5$ and $r = 10$, namely the time to the most recent common ancestor (A), stemminess (B), number of multimerers (C) and the size of the largest multimerger (D).

238 Note that in Equation 30 the term $\binom{n_i}{k_i}$ term from the coalescent rate cancels out with its reciprocal
 239 from the probability of sampling k_i specific lineages to coalesce within a set of n_i . Estimating the
 240 lambda measure in general is a difficult problem (Koskela 2018; Miró Pina et al. 2023). Here however
 241 we focus on estimation under the omega-coalescent model, where the $\lambda_{n,k}$ terms are given by Equation
 242 28. There are therefore two parameters to estimate which have direct and important biological
 243 meaning: the effective population size N_t (which remains constant) and the dispersion parameter
 244 r of the Negative-Binomial offspring distribution. We perform estimation simply by maximising the
 245 likelihood in Equation 30, using the Brent algorithm (Brent 1971) when estimating a single parameter
 246 and the L-BFGS-B algorithm when (Byrd et al. 1995) estimating both parameters.

247 We simulated 100 genealogies from the omega-coalescent model each of which had $n = 100$ leaves, with
 248 parameter N_e drawn uniformly at random between 100 and 500 and parameter r drawn uniformly at
 249 random between 0.01 and 2. If we assume knowledge of the dispersion parameter, then estimating
 250 the population size works really well (Figure 6A). Conversely we obtain good result when estimating
 251 the dispersion parameter given a known population size (Figure 6B). However, attempting to estimate
 252 both parameters at the same time performed significantly less well (Figures 6C and D). To illustrate
 253 the cause of this, we consider a simulation for which the true N_t was 200 and the true r was 0.5, and
 254 we construct the likelihood surface (Figure 6E). This shows a strong inverse tradeoff between the two
 255 parameters, which explains why one can be estimated given the other, but not jointly.

256 8 Implementation

257 We implemented the analytical methods described in this paper in a new R package entitled *EpiLambda*
 258 which is available at <https://github.com/xavierdidelot/EpiLambda> for R version 3.5 or later. All
 259 code and data needed to replicate the results are included in the “run” directory of the *EpiLambda*
 260 repository. The R package **ape** was used to store, manipulate and visualise phylogenetic trees (Paradis
 261 and Schliep 2019).

262 9 Discussion

263 The omega-coalescent could be extended to allow temporally offset leaves following work on the
 264 coalescent (Drummond et al. 2003) and the beta-coalescent (Hoscheit and Pybus 2019). It could

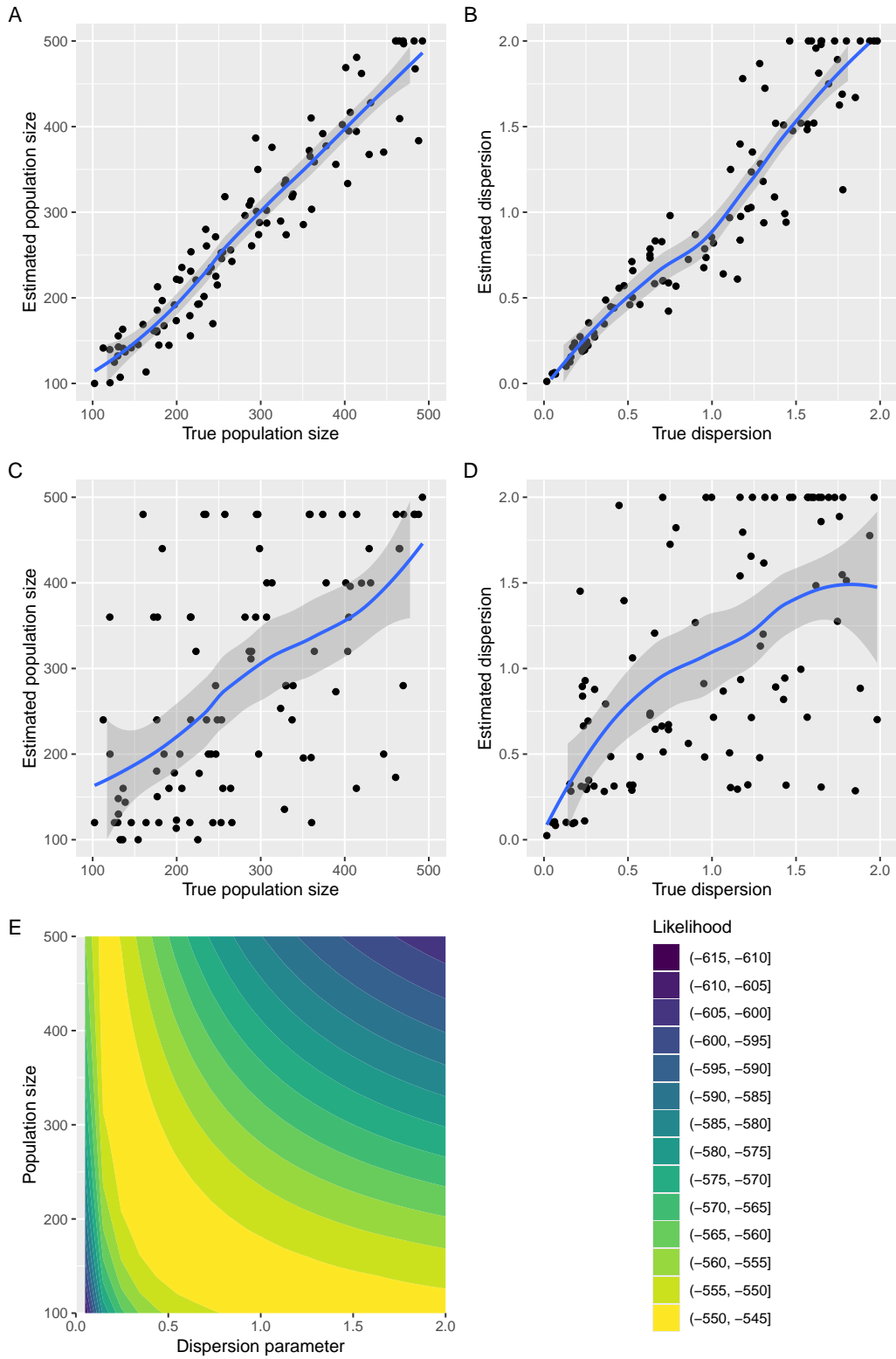


Figure 6: Maximum likelihood estimation of parameters. (A) Estimation of the population size given the dispersion parameter. (B) Estimation of the dispersion parameter given the population size. (C and D) Joint estimation of both the population size and dispersion parameters. (E) Example of likelihood surface as a function of both parameters.

also be defined in a varying population size following the same approach as previously described for the coalescent (Griffiths and Tavaré 1994; Pybus et al. 2000; Ho and Shapiro 2011) and the beta-coalescent (Hoscheit and Pybus 2019; Zhang and Palacios 2024). This could be even more useful for the omega-coalescent than for the beta-coalescent since in the omega-coalescent the probability of multimerger events of various size depends explicitly on the population size (see for example Figure 3).

We compared the omega-coalescent only to the beta-coalescent (Schweinsberg 2003) but it could also be compared to the Dirac coalescent aka psi-coalescent (Eldon and Wakeley 2006), the Durrett-Schweinsberg coalescent (Durrett and Schweinsberg 2005) or the extended Beta-coalescent (Helekal et al. 2025).

The xi-coalescent models admit multiple simultaneous mergers (Schweinsberg 2000).

Difference between transmission tree and phylogenetic tree (Jombart et al. 2011). Modelling within-host evolution to bridge the gap (Didelot et al. 2014; Hall et al. 2015; Didelot et al. 2017). Superspreading individuals vs superspreading events (Riley et al. 2003; Wallinga and Teunis 2004; Ho et al. 2023).

Acknowledgements

We acknowledge funding from the National Institute for Health Research (NIHR) Health Protection Research Unit in Genomics and Enabling Data.

References

- Anderson, R.M., May, R.M., 1991. *Infectious Diseases of Humans: Dynamics and Control*. Oxford University Press, USA.
- Brent, R.P., 1971. An algorithm with guaranteed convergence for finding a zero of a function. *The computer journal* 14, 422–425.
- Byrd, R.H., Lu, P., Nocedal, J., Zhu, C., 1995. A limited memory algorithm for bound constrained optimization. *SIAM Journal on scientific computing* 16, 1190–1208.
- Cannings, C., 1974. The latent roots of certain Markov chains arising in genetics: a new approach, I. Haploid models. *Adv. Appl. Probab.* 6, 260–290. doi:10.2307/1426293.
- Didelot, X., Fraser, C., Gardy, J., Colijn, C., 2017. Genomic infectious disease epidemiology in partially sampled and ongoing outbreaks. *Molecular Biology and Evolution* 34, 997–1007. doi:10.1093/molbev/msw275.
- Didelot, X., Gardy, J., Colijn, C., 2014. Bayesian inference of infectious disease transmission from whole genome sequence data. *Molecular Biology and Evolution* 31, 1869–1879. doi:10.1093/molbev/msu121.
- Donnelly, P., Kurtz, T.G., 1999. Particle Representations for Measure-Valued Population Models. *The Annals of Probability* 27. doi:10.1214/aop/1022677258.
- Drummond, A.J., Pybus, O.G., Rambaut, A., Forsberg, R., Rodrigo, A.G., 2003. Measurably evolving populations. *Trends in Ecology and Evolution* 18, 481–488. doi:10.1016/S0169-5347(03)00216-7.
- Du, Z., Wang, C., Liu, C., Bai, Y., Pei, S., Adam, D.C., Wang, L., Wu, P., Lau, E.H.Y., Cowling, B.J., 2022. Systematic review and meta-analyses of superspreading of SARS-CoV-2 infections. *Transboundary and Emerging Diseases* 69. doi:10.1111/tbed.14655.
- Durrett, R., Schweinsberg, J., 2005. A coalescent model for the effect of advantageous mutations on the genealogy of a population. *Stochastic Processes and their Applications* 115, 1628–1657. doi:10.1016/j.spa.2005.04.009.
- Eldon, B., Wakeley, J., 2006. Coalescent Processes When the Distribution of Offspring Number Among Individuals Is Highly Skewed. *Genetics* 172, 2621–2633. doi:10.1534/genetics.105.052175.
- Ferguson, N.M., Cummings, D.A.T., Fraser, C., Cajka, J.C., Cooley, P.C., Burke, D.S., 2006. Strategies for mitigating an influenza pandemic. *Nature* 442, 448–452. doi:10.1038/nature04795.

312 Fisher, R.A., 1930. The genetical theory of natural selection. Clarendon Press. doi:10.5962/bh1.
313 title.27468.

314 Fraser, C., Li, L.M., 2017. Coalescent models for populations with time-varying population sizes and
315 arbitrary offspring distributions. bioRxiv , 10.1101/131730doi:10.1101/131730.

316 Fraser, C., Riley, S., Anderson, R.M., Ferguson, N.M., 2004. Factors that make an infectious
317 disease outbreak controllable. Proceedings of the National Academy of Sciences 101, 6146–6151.
318 doi:10.1073/pnas.0307506101.

319 Gómez-Carballa, A., Pardo-Seco, J., Bello, X., Martínón-Torres, F., Salas, A., 2021. Superspreading
320 in the emergence of COVID-19 variants. Trends in Genetics 37, 1069–1080. doi:10.1016/j.tig.
321 2021.09.003.

322 Grassly, N.C., Fraser, C., 2008. Mathematical models of infectious disease transmission. Nature
323 Reviews Microbiology 6, 477–87. doi:10.1038/nrmicro1845.

324 Griffiths, R.C., Tavaré, S., 1994. Sampling theory for neutral alleles in a varying environment.
325 Philosophical Transactions of the Royal Society B 344, 403–410.

326 Hall, M., Woolhouse, M., Rambaut, A., 2015. Epidemic Reconstruction in a Phylogenetics Framework:
327 Transmission Trees as Partitions of the Node Set. PLOS Computational Biology 11, e1004613.
328 doi:10.1371/journal.pcbi.1004613.

329 Heledkal, D., Koskela, J., Didelot, X., 2025. Inference of multiple mergers while dating a pathogen
330 phylogeny. Systematic Biology , in press.

331 Ho, F., Parag, K.V., Adam, D.C., Lau, E.H.Y., Cowling, B.J., Tsang, T.K., 2023. Accounting for the
332 Potential of Overdispersion in Estimation of the Time-varying Reproduction Number. Epidemiology
333 34, 201–205. doi:10.1097/EDE.0000000000001563.

334 Ho, S.Y.W., Shapiro, B., 2011. Skyline-plot methods for estimating demographic history from
335 nucleotide sequences. Molecular Ecology Resources 11, 423–434. doi:10.1111/j.1755-0998.2011.
336 02988.x.

337 Hoscheit, P., Pybus, O.G., 2019. The multifurcating skyline plot. Virus Evolution 5, 1–10.
338 doi:10.1093/ve/vez031.

339 Jombart, T., Eggo, R.M., Dodd, P.J., Balloux, F., 2011. Reconstructing disease outbreaks from genetic
340 data: A graph approach. Heredity 106, 383–90. doi:10.1038/hdy.2010.78.

341 Keeling, M.J., Rohani, P., 2008. Modeling infectious diseases in humans and animals. Princeton
342 university press.

343 Kingman, J., 1982a. The coalescent. *Stochastic Processes and their Applications* 13, 235–248.
344 doi:10.1016/0304-4149(82)90011-4.

345 Kingman, J.F.C., 1982b. On the genealogy of large populations. *Journal of Applied Probability* 19,
346 27–43. doi:10.2307/3213548.

347 Koelle, K., Rasmussen, D.A., 2012. Rates of coalescence for common epidemiological models at
348 equilibrium. *Journal of The Royal Society Interface* 9, 997–1007. doi:10.1098/rsif.2011.0495.

349 Koskela, J., 2018. Multi-locus data distinguishes between population growth and multiple merger
350 coalescents. *Statistical Applications in Genetics and Molecular Biology* 17, 1–24. doi:10.1515/
351 sagmb-2017-0011.

352 Kucharski, A.J., Althaus, C.L., 2015. The role of superspreading in Middle East respiratory syndrome
353 coronavirus (MERS-CoV) transmission. *Eurosurveillance* 20. doi:10.2807/1560-7917.ES2015.20.
354 25.21167.

355 Lemieux, J.E., Siddle, K.J., Shaw, B.M., Loreth, C., Schaffner, S.F., Gladden-Young, A., Adams,
356 G., Fink, T., Tomkins-Tinch, C.H., Krasilnikova, L.A., DeRuff, K.C., Rudy, M., Bauer, M.R.,
357 Lagerborg, K.A., Normandin, E., Chapman, S.B., Reilly, S.K., Anahtar, M.N., Lin, A.E., Carter,
358 A., Myhrvold, C., Kembell, M.E., Chaluvadi, S., Cusick, C., Flowers, K., Neumann, A., Cerrato,
359 F., Farhat, M., Slater, D., Harris, J.B., Branda, J.A., Hooper, D., Gaeta, J.M., Baggett, T.P.,
360 O’Connell, J., Gnirke, A., Lieberman, T.D., Philippakis, A., Burns, M., Brown, C.M., Luban, J.,
361 Ryan, E.T., Turbett, S.E., LaRocque, R.C., Hanage, W.P., Gallagher, G.R., Madoff, L.C., Smole, S.,
362 Pierce, V.M., Rosenberg, E., Sabeti, P.C., Park, D.J., MacInnis, B.L., 2021. Phylogenetic analysis
363 of SARS-CoV-2 in Boston highlights the impact of superspreading events. *Science* 371, eabe3261.
364 doi:10.1126/science.abe3261.

365 Li, L.M., Grassly, N.C., Fraser, C., 2017. Quantifying Transmission Heterogeneity Using Both
366 Pathogen Phylogenies and Incidence Time Series. *Molecular Biology and Evolution* 34, 2982–2995.
367 doi:10.1093/molbev/msx195.

368 Lloyd-Smith, J., Schreiber, S., Kopp, P., Getz, W., 2005. Superspreading and the effect of individual
369 variation on disease emergence. *Nature* 438, 355–9. doi:10.1038/nature04153.

370 Menardo, F., Gagneux, S., Freund, F., 2021. Multiple Merger Genealogies in Outbreaks of
371 *Mycobacterium tuberculosis*. *Molecular Biology and Evolution* 38, 290–306. doi:10.1093/molbev/
372 msaa179.

373 Miró Pina, V., Joly, É., Siri-Jégousse, A., 2023. Estimating the Lambda measure in multiple-merger
374 coalescents. *Theoretical Population Biology* 154, 94–101. doi:10.1016/j.tpb.2023.09.002.

375 Moran, P., 1958. Random Processes in Genetics. *Mathematical Proceedings of the Cambridge*
376 *Philosophical Society* 54, 60–71.

377 Paradis, E., Schliep, K., 2019. Ape 5.0: An environment for modern phylogenetics and evolutionary
378 analyses in R. *Bioinformatics* 35, 526–528. doi:10.1093/bioinformatics/bty633.

379 Pitman, J., 1999. Coalescents with multiple collisions. *The Annals of Probability* 27, 1870–1902.

380 Potts, R.B., 1953. Note on the Factorial Moments of Standard Distributions. *Australian Journal of*
381 *Physics* 6, 498–499. URL: <https://www.publish.csiro.au/ph/ph530498>, doi:10.1071/ph530498.
382 publisher: CSIRO PUBLISHING.

383 Pybus, O.G., Rambaut, A., Harvey, P.H., 2000. An integrated framework for the inference of viral
384 population history from reconstructed genealogies. *Genetics* 155, 1429–1437. doi:10.1073/pnas.
385 88.5.1597.

386 Riley, S., Fraser, C., a Donnelly, C., Ghani, A.C., Abu-Raddad, L.J., Hedley, A.J., Leung, G.M.,
387 Ho, L.M., Lam, T.H., Thach, T.Q., Chau, P., Chan, K.P., Lo, S.V., Leung, P.Y., Tsang, T., Ho,
388 W., Lee, K.H., Lau, E.M.C., Ferguson, N.M., Anderson, R.M., 2003. Transmission dynamics of the
389 etiological agent of SARS in Hong Kong: Impact of public health interventions. *Science* 300, 1961–6.
390 doi:10.1126/science.1086478.

391 Sagitov, S., 1999. The general coalescent with asynchronous mergers of ancestral lines. *Journal of*
392 *Applied Probability* 36, 1116–1125. doi:10.1239/jap/1032374759.

393 Schweinsberg, J., 2000. Coalescents with Simultaneous Multiple Collisions. *Electronic Journal of*
394 *Probability* 5. doi:10.1214/EJP.v5-68.

395 Schweinsberg, J., 2003. Coalescent processes obtained from supercritical Galton–Watson processes.
396 *Stochastic Processes and their Applications* 106, 107–139. doi:10.1016/S0304-4149(03)00028-0.

397 Stein, R.A., 2011. Super-spreaders in infectious diseases. *International Journal of Infectious Diseases*
398 15, e510–e513. doi:10.1016/j.ijid.2010.06.020.

399 Tripathi, R.C., Gupta, R.C., Gurland, J., 1994. Estimation of parameters in the beta binomial model.
400 *Annals of the Institute of Statistical Mathematics* 46, 317–331. URL: [https://doi.org/10.1007/](https://doi.org/10.1007/BF01720588)
401 [BF01720588](https://doi.org/10.1007/BF01720588), doi:10.1007/BF01720588.

- Volz, E.M., 2012. Complex population dynamics and the coalescent under neutrality. *Genetics* 190, 187–201. doi:10.1534/genetics.111.134627.
- Wallinga, J., Teunis, P., 2004. Different Epidemic Curves for Severe Acute Respiratory Syndrome Reveal Similar Impacts of Control Measures. *American Journal of Epidemiology* 160, 509–516.
- Wang, J., Chen, X., Guo, Z., Zhao, S., Huang, Z., Zhuang, Z., Wong, E.L.y., Zee, B.C.Y., Chong, M.K.C., Wang, M.H., Yeoh, E.K., 2021. Superspreading and heterogeneity in transmission of SARS, MERS, and COVID-19: A systematic review. *Computational and Structural Biotechnology Journal* 19, 5039–5046. doi:10.1016/j.csbj.2021.08.045.
- Wang, L., Didelot, X., Yang, J., Wong, G., Shi, Y., Liu, W., Gao, G.F., Bi, Y., 2020. Inference of person-to-person transmission of COVID-19 reveals hidden super-spreading events during the early outbreak phase. *Nature Communications* 11, 5006. doi:10.1038/s41467-020-18836-4.
- Woolhouse, M.E.J., Dye, C., Etard, J.F., Smith, T., Charlwood, J.D., Garnett, G.P., Hagan, P., Hii, J.L.K., Ndhlovu, P.D., Quinnell, R.J., Watts, C.H., Chandiwana, S.K., Anderson, R.M., 1997. Heterogeneities in the transmission of infectious agents: Implications for the design of control programs. *Proceedings of the National Academy of Sciences* 94, 338–342. doi:10.1073/pnas.94.1.338.
- Wright, S., 1931. Evolution in Mendelian populations. *Genetics* 16, 97–159. doi:10.1093/genetics/16.2.97.
- Zhang, J., Palacios, J.A., 2024. Multiple merger coalescent inference of effective population size. *arXiv*, 2407.14976doi:10.48550/arXiv.2407.14976, arXiv:2407.14976.